J. At. Mol. Sci.
doi: 10.4208/jams.072415.082615a

Vol. **6**, No. 3, pp. 155-163
September 2015

Theoretical study of stereodynamics for the S+H_2 (v=0-2, j=0) $\rightarrow$ SH+H reaction

Yanlei Liu, Hongsheng Zhai, and Yufang Liu*

College of Physics and Electronical Engineering, Henan Normal University, Xinxiang 453007, China

Received 24 July 2015; Accepted (in revised version) 26 August 2015
Published Online 30 September 2015

Abstract. Quasi-classical trajectory (QCT) calculations for the reaction S+H_2(v=0-2, j=0)$\rightarrow$SH+H have been performed in order to investigate the effect of initial vibrational states on both the scalar and vector properties. The integral cross sections, opacity function have been calculated. The results indicate that the reaction probability and the cross section increase as the initial vibrational quantum number increases. The vibrational distributions and rotational distributions at different vibrational excited states are presented, and the results are discussed in detail. In addition, the vector properties, involving scattering directions of reaction product and the alignment and orientation of rotational angular momentum, are calculated and discussed. The results indicate that the vibrational excited states have a positive effect on the forward scattering direction of the product, and the vibrational excited states have slight effect on the alignment and orientation of the rotational angular momentum.

PACS: 31.15.xv, 34.35.+a

Key words: quasi-classical trajectory, integral cross section, ro-vibrational distribution, vector correlation.

1 Introduction

The combustion reaction of sulphur with hydrogen has abstracted extensive attention because of its important role in the atmospheric chemistry and air contamination. The reaction S+H_2 is the simplest reaction involving the sulphur atom. The investigation on the reaction S+H_2 might reveal microscopic mechanism of A+BC reaction. Therefore, both theoretical [1-9] and experimental [10, 11] studies on the title reaction have been reported.

*Corresponding author. *Email address:* yf-liu@htu.cn (Y. F. Liu)

Maiti *et al.* [4] studied the intersystem crossing effect in the S+H_2 reaction by employing a "mixed" representation approach in combination with a trajectory surface-hopping method. Klos *et al.* [6] reported their theoretical study of the S(^{1}D)+$H_2/D_2 \rightarrow$ SH+H/SD+D, including the nonadiabatic effect. Berteloite *et al.* [7] performed kinetics and crossed-beam experiments in conditions approaching the cold energy regime, and Lee and Liu [10, 11] investigated the S(^{1}D) + H_2 reaction and its isotopic variants through Doppler-selected time-of-flight detection of the H or D product. An accurate *ab initio* potential energy surface (PES) for the lowest triplet state of H_2S was reported by Lv *et al.* [12], which makes it possible for us to study the vector properties of the reaction.

As mentioned above, most of the investigations on the reaction S+HH basically deal with the scalar properties. It is well known that the vector properties can reveal the details of the reaction with space information. To our best knowledge, only one study has been reported concerning the vector properties of the reaction S+H_2. Li *et al.* [13] investigated the effect of collision energy on the stereodynamics of the reaction S+HH/HD/DH/DD. They calculated the cross sections and vector properties at different collision energies. However the effect of vibrational excited states was not involved in their study.

In this paper, we calculated both the scalar and vector properties of the reaction S+H_2 at different initial vibrational excited states. The QCT method was present in Section 2; the result and discussion were present in Section 3; the conclusion was showed in Section 4.

2 Quasi-classical trajectory method

The quasi-classical trajectory (QCT) method employed in this study is the same as the method has been expressed particularly in previous works [14-26], we only present the calculation details of the current work. In our calculation, the classical Hamilton's equations are numerically integrated for motion in three dimensions, and the accuracy of the calculation is verified by checking the conservation of both the total energy and angular momentum. Batches of 100 000 trajectories have been run at each vibrational excited state. The integrate cross section (ICS) is calculated by $\sigma = \pi b_{\max}^2 p_r$, in which p_r represents the reaction probability, is given by N_r/N_t, where N_r and N_t represent the number of reaction trajectories and total trajectory number (100 000) respectively.

The center-of-mass (CM) frame [24-26] is chosen to describe the vector correlation, and its details are specified as follows. As can be seen in Fig. 1, k means the reactant relative velocity parallel to the z-axis, and k' is the product relative velocity. The x-z plane, containing vectors k and k', is the scattering plane. θ_t represents the angle between k and k', which indicates the scattering direction of the product. j' is the rotational angular momentum of product, whose polar and azimuthal angles are θ_r and ϕ_r, respectively. $P(\theta_r)$ and $P(\phi_r)$ describe the probability density distribution of reaction products, reflecting $k-j'$ and $k-k'-j'$ vector-correlation respectively. The alignment and orientation of j' can be obtained by analyzing and $P(\theta_r)$ and $P(\phi_r)$ distributions. Four generalized

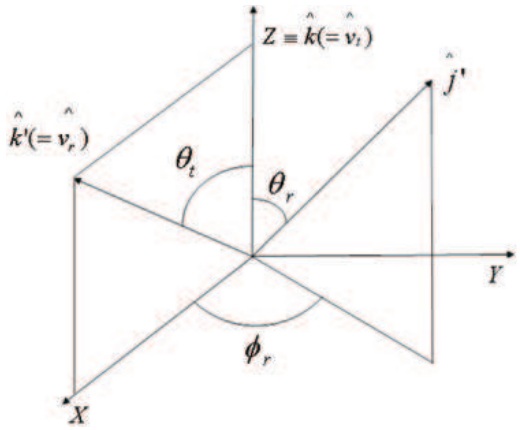

Figure 1: The center-of-mass coordinate system used to describe the k,k' and j' correlation.

polarization-dependent differential cross-sections (PDDCSs) are used to describe the full three-dimensional angular distribution associated with $k-k'-j'$ correlation in the CM frame. The fully correlated center-of-mass angular distribution is written as [14, 18]:

$$P(\omega_t,\omega_r)=\frac{1}{2}\sum_{kq}\frac{[k]}{4\pi}\frac{1}{\sigma}\frac{d\sigma_{kq}}{d\omega_t}c_{kq}(\theta_r,\phi_r)^* \tag{1}$$

where $[k]$=2k+1, $(1/\sigma)(d\sigma_{kq}/d\omega_t)$, is the generalized polarization-dependent differential cross section (PDDCS) and $c_{kq}(\theta_r, \phi_r)$ are the modified spherical harmonics. The PDDCS is written in the following form:

$$\frac{1}{\sigma}\frac{d\sigma_{kq\pm}}{d\omega_t}=\sum_{k_1}\frac{k_1}{4\pi}S^{k_1}_{kq\pm}C_{k_1q}(\theta_t, 0) \tag{2}$$

where the $S^{k_1}_{kq\pm}$ is evaluated by the expected value expression,

$$S^{k_1}_{kq\pm}=\langle c_{k_1q}(\theta_t, 0)c_{kq}(\theta_r, 0)[(-1)^q e^{iq\phi_r}\pm e^{-iq\phi_r}]\rangle \tag{3}$$

where the angular brackets represent an average over all angles.

The different cross section is given by

$$\frac{1}{\sigma}\frac{d\sigma_{00}}{d\omega_t}\equiv P(\omega_t)=\sum_{k_1}\frac{k_1}{4\pi}h^{k_1}_0(k_1,0)P_{k_1}(\cos\theta_t) \tag{4}$$

The function $f(\theta_r)$ can be expanded in a set of Legendre polynomials [14, 23]

$$f(\theta_r)=\sum_l a_l p_l(\cos\theta_r). \tag{5}$$

Thus, l=2 indicates the product rotational alignment.

Where, P_2 is a second Legendre moment, and the brackets show an average over the distribution of j' about k.

$$\langle P_2(j'\cdot k)\rangle = \frac{1}{2}\langle 3\cos^2\theta - 1\rangle. \tag{6}$$

The $P(\theta_r)$ distribution can be expanded in a serious of Legendre polynomials [17,23] as:

$$P(\theta_r) = \frac{1}{2}\sum_k [k] a_0^k P_k(\cos\theta_r) \tag{7}$$

$$a_0^k = \langle P_k(\cos\theta_r)\rangle. \tag{8}$$

The expanding coefficient a_0^k are called orientation (k is odd) and alignment (k is even) parameter.

The dihedral angle distribution $P(\theta_r)$ can be expanded in Fourier series [18, 23]

$$P(\phi_r) = \frac{1}{2\pi}[1 + \sum_{neven\geq 2} a_n \cos n\phi_r + \sum_{nodd\geq 1} b_n \sin n\phi_r] \tag{9}$$

$$a^n = 2\langle \cos n\phi_r\rangle \quad b^n = 2\langle \sin n\phi_r\rangle.$$

3 Results and discussion

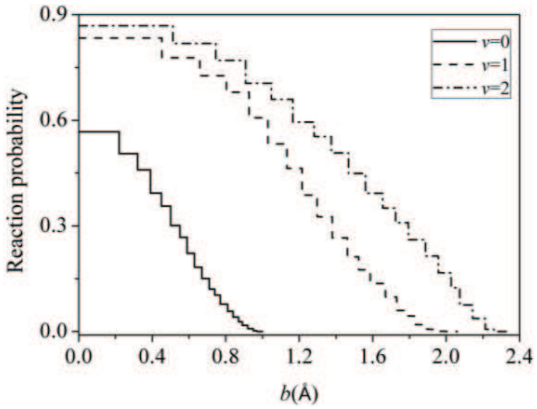

Figure 2: Total reaction probability as a function of the impact parameter b at three vibrational excited states for the reaction S+H_2(v=0-2, j=0)→SH+H.

The opacity function is the reaction probability as a function of the impact parameter b, provides an initial understanding of the title reaction. Fig. 2 shows the QCT opacity function for the reaction S+H_2(v=0-2, j=0)→SH+H at three vibrational excited states. It is clearly can be seen that the reaction probability slowly decreases as b increases for all the three initial vibrational excited states. This means that the huge impact parameter

Table 1: The reaction probability, maximum impact parameter and integrate cross section of the reacation S+H_2(v=0-2, j=0)→SH+H at three vibrational excited states.

v	P_r	b_{max}(Å)	ICS(Å^2)
0	0.19	1.44	1.26
1	0.32	2.04	4.23
2	0.39	2.33	6.70

may minish the probability of the reactive collisions. For a given impact parameter, the reaction probability increases with the increase of initial vibrational quantum number v. The maximum impact parameter b_{max} increases obviously with v increases. This will have a considerable effect on the integral cross section since it are given by $\sigma = \pi b_{max}^2 p_r$.

In order to present the effect of vibrational excited state on the reaction probability and integrate cross section clearly. We list the the reaction probability, maximum impact parameter and integrate cross section of the reacation S+H_2(v=0-2, j=0)→SH+H at three vibrational excited states in Table 1. Clearly, both total reaction probability and integrate cross section increase sharply with the increase of initial vibrational quantum number v. The results indicate that the vibrational excited state has a positive influence on the title reaction.

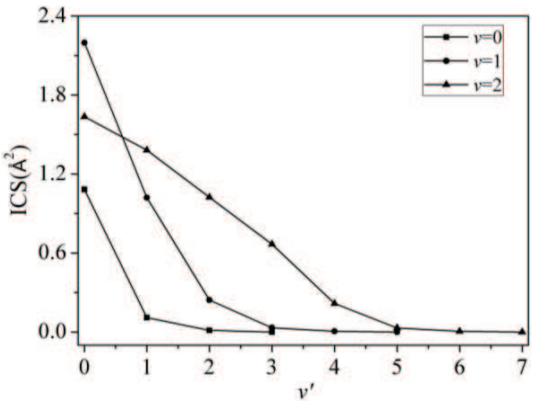

Figure 3: Product vibrational distributions at three vibrational excited states for the reaction S+H_2(v=0-2, j=0)→SH+H.

Fig. 3 shows the product vibrational distribution, i.e. the ICS as a function of the product vibrational quantum number v' of SH, at different vibrational excited states for reaction S+H_2(v=0-2, j=0)→SH+H. The vibrational excitation of HS increases when initial vibrational quantum number v increases. For v=0, the most population vibrational state is v'=0 and ICS decreases rapidly with the increase of v'. The shape of the vibrational distributions at v=1 is similar with that at v=0. Although the most population vibration state at v=2 is v'=0, the ICS of v=2 at v'=0 is smaller than that of v=1. The ICS decreases slowly with v' increasing. It can be concluded that, the reactions which produce SH with

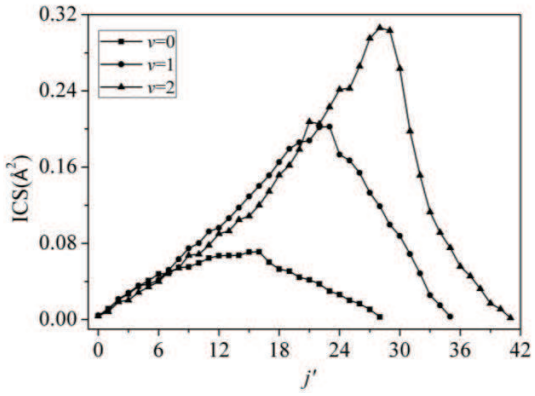

Figure 4: Product rotational distributions at three vibrational excited states for the reaction S+H_2(v=0-2, j=0)→SH+H.

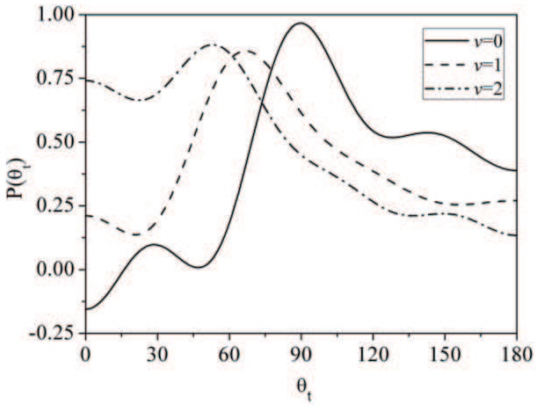

Figure 5: The distribution of $P(\theta_t)$ at three vibrational excited states for the reaction S+H_2(v=0-2, j=0)→SH+H.

high vibrational states are restrained. This may be attributed to the repulsive potential energy surface, in which the collision energy mainly be transformed to the translational energy of the product. In addition, the initial vibrational excitation produce molecular with high vibrational states indicates that it plays a positive role in the reaction.

The product rotational distribution, i.e. the ICS as a function of the rotation quantum j' of SH, is shown in Fig. 4. We can see that the maximum rotational quantum number of SH increases from j'=28 to j'=41 as vibrational quantum number v' increases. For v=0, the ICS increases slowly and reaches the peak at about j'=15 then decreases to a tiny value slowly. When comes to v=1 and v=2, the shapes the product rotational distribution are similar with that of v=0. The ICSs of v=1 and v=2 change more quickly than that of v=0. The value of the peak of product rotational distribution increases with v increasing, and the peak moves to the larger j' when v increases. The results indicate that the initial vibrational excitation promote the reaction, which produce molecular with high rotational states.

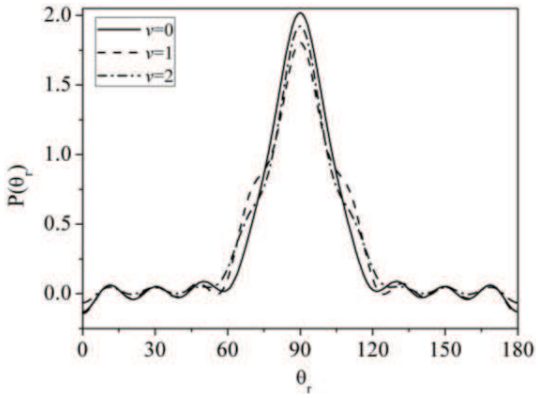

Figure 6: The distribution of $P(\theta_r)$ at three vibrational excited states for the reaction S+H_2(v=0-2, j=0)→SH+H.

The polarization dependent generalized cross-sections (PDDCSs) for the title reaction at three vibrational excited states are shown in Fig. 5, which reflect the $k-k'-j'$ correlations. The $P(\theta_t)$ distribution, i.e. PDDCS$(2\pi/\sigma)(d\sigma_{00}/d\omega_t)$, describes the scattering directions of the product. For v=0, the peak of $P(\theta_t)$ distribution appears at θ_t=90°. The value of the $P(\theta_t)$ distribution for θ_t >90° is higher than that for θ_t <90°. This means that the sideway and backward scattering dominate the title reaction at v=0. The peak of $P(\theta_t)$ distribution at v=1 moves to θ_t=60°. The forward scattering become stronger and the backward scattering become weaker. In terms of v=2, it is clearly can be seen that the forward scattering dominate the title reaction. The results indicate that the vibrational excitation play an important role in the scattering direction of the product SH. The vibrational excitation has a positive influence on the forward scattering of the product molecular.

Fig. 6 shows the $P(\theta_r)$ distributions for the reaction S+H_2(v=0-2, j=0)→SH+H at three vibrational excited states. For all the three states, the $P(\theta_r)$ distributions exhibit a maximum at θ_r=90° and are symmetric about θ_r=90°. These means that the product rotational angular momentum vector j' is strongly aligned along the direction perpendicular to the k vector. The peak of $P(\theta_r)$ distribution of becomes lower when the vibrational quantum number v from 0 to 1, while the peak becomes higher when v increases from 1 to 2. Just as shown in Fig. 6, the peaks of the three vibrational excited states are close to each other. This means the vibrational excitation has slight influence on the alignment of the product rotational angular momentum vector j'. The alignment parameters $\langle P_2(j'\cdot k)\rangle$ are calculated, which give a simple way to express the degree of the product rotational alignment effect. The value of $\langle P_2(j'\cdot k)\rangle$ for v=0-2 are -0.4965, -0.4936 and -0.4938 respectively. The change tendency of product rotational alignment parameter $\langle P_2(j'\cdot k)\rangle$ is in agreement with the distributions of $P(\theta_r)$.

Fig. 7 shows the $P(\phi_r)$ distribution for the reaction S+H_2(v=0-2, j=0)→SH+H at three vibrational excited states. In all case, the $P(\phi_r)$ distributions are asymmetric with respect

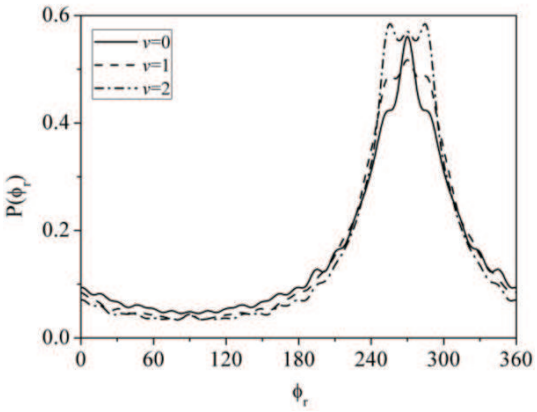

Figure 7: The distribution of $P(\phi_r)$ at three vibrational excited states for the reaction S+H_2(v=0-2, j=0)→SH+H.

to ϕ_r=180°, with slow peaks appearing at ϕ_r=270°. This means a obvious preference for orientation along the negative y-axis. The $P(\phi_r)$ distribution is in good agreement with the result obtained by Han *et al.* [14] that the distribution of j' does not have azimuthal asymmetry for the H+LL mass combination on the repulsive potential energy surface. The orientation of SH for the title reaction may results from the repulsive energy between two H atoms, which leads to the violation of the symmetry during the reaction. According to the repulsive model about the reaction A+BC, the product rotational angular momentum vector can be expressed by $j' = L\sin^2\beta + j\cos^2\beta + J_1 m_B/m_{AB}$. Where L is the reagent orbital angular momentum and j is the reagent rotational angular moment; where is the mass factor and calculated by $\cos^2\beta = m_A m_C/(m_A+m_B)(m_B+m_C)$. $J_1 = \sqrt{\mu_{BC}R}(r_{AB}\times r_{CB})$, r_{AB} and r_{CB} are unit vectors, where B point to A and C; μ_{BC} is reduce mass of BC and R is the repulsive energy. During the chemical-bond breaking and forming for the title reaction, the term $L\sin^2\beta + j\cos^2\beta$ is symmetric. The term $J_1 m_B/m_{AB}$ shows a preferential direction because of the repulsive energy, which leads the orientation of the product SH. In addition, from Fig. 7, we can obtain that the vibrational excitation has slight influence on the orientation of the product SH for the title reaction.

4 Conclusion

Quasi-classical trajectory (QCT) calculations for the reaction S+H_2(v=0-2, j=0)→SH+H have been performed based on the potential energy surface constructed by Lv *et al.* The scalar properties involving reaction probability, the integral cross sections and opacity function have been shown and the calculated parameter bmax are shown. The results indicate that both the reaction probability and the integrate cross section increase obviously as the initial vibrational quantum number increases. The vibrational distributions and rotational distributions for the title reaction are shown. The results indicate that the vibrational excitation has a positive influence on the reaction and promotes the reaction,

which produce molecular with high vibrational and rotational states. The vector properties, involving scattering directions of reaction product and the alignment and orientation of rotational angular momentum, are also presented. The result can be concluded: a) sideway and backward scattering dominate the reaction at v=0, while the vibrational excitation has a positive influence on the forward scattering; b) the rotational angular momentum of the product SH is strongly aligned along the direction perpendicular to the k vector and orientates along the negative y-axis; c) the vibrational excitation has slight effect on the alignment and orientation of the rotational angular momentum j'.

Acknowledgments. This work is supported by the Innovation Scientists and Technicians Troop Construction Projects of Henan Province (Grant No. 124200510013).

References

[1] B. S. Sengupta, L. Curtiss, J. R. Miller, J. Chem. Phys. 104 (1996) 9888.
[2] H. Shiina, M. Oya, K. Yamashita, A. Miyoshi, H. Matsui J. Phys. Chem. 100 (1996) 2136.
[3] H. Shiina, A. Miyoshi, H. Matsui, J. Chem. Phys. A 102 (1998) 3556.
[4] B. Maiti, G. C. Schatz, G. Lendvay, J. Chem. Phys. A 108 (2004) 8772.
[5] L. Banares, J. F. Castillo, P. Honvault, J. M. Launay, Phys. Chem. Chem. Phys. 7 (2005) 627.
[6] J. A. Klos, P. J. Dagdigian, M. H. Alexander, J. Chem. Phys. 127 (2007) 154321.
[7] C. Berteloite, M. Lara, A. Bergeat, S. D. Le Picard, Dayou F, K. M. Hickson, A. Canosa, C. Naulin, J. M. Launay, I. R. Sims, M. Costes, Phys. Rev. Lett. 105 (2010) 203201.
[8] M. Lara, F. Dayou, J. M. Launay, Phys. Chem. Chem. Phys. 13 (2011) 8359.
[9] M. Lara, P. G. Jambrina, A. C. J. Varandas, J. M. Launay, F. Aoiz, J. Chem. Phys. 135 (2011) 134313.
[10] S. H. Lee, K. Liu, Chem. Phys. Lett. 290 (1998) 323.
[11] S. H. Lee, K. Liu, Appl. Phys. B: Lasers 71 (2000) 627.
[12] S. J. Lv, P. Y. Zhang, K. L. Han, G. Z. He, J. Chem. Phys. 136 (2012) 94308.
[13] M. Li, H. S. Zhai, Y. L. Liu, Journal of Henan Normal University 42 (2014) 50.
[14] M. D. Chen, K. L. Han, N. Q. Lou, Chem. Phys. Lett. 357 (2002) 483.
[15] R. L. Martin, Chem. Phys. 82 (1983) 337.
[16] S. J. Lu, P. Y. Zhang , K. L. Han, G. Z. He, J. Chem. Phys. 136 (2012) 94308.
[17] K. L. Han, G. Z. He, N. Q .Lou, J. Chem. Phys. 105 (1996) 8699.
[18] M. L. Wang, K. L. Han, G. Z. He, J. Chem. Phys. 109 (1998) 5446.
[19] M. L. Wang, K. L. Han, G. Z. He, J. Chem. Phys. A 102 (1998) 10204.
[20] M. Karplus, R. Porter, R. Sharma, J. Chem. Phys. 43 (1965) 3259.
[21] M. G. Prisant, C. T. Rettner, R. N. Zare, J. Chem. Phys. 75 (1981) 2222.
[22] N. E. Shafer-Ray, A. J. Orr-Ewing, R. N. Zare, J. Phys. Chem. 99 (1995) 7591.
[23] F. Aoiz, M. Brouard, P. Enriquez, J. Chem. Phys. 105 (1996) 4964.
[24] N. H. Hijazi, J. C. Polanyi, J. Chem. Phys. 63 (1975) 2249.
[25] N. H. Hijazi, J. C. Polanyi, Chem. Phys. 11 (1975) 1.
[26] K. L. Han, G. Z. He, N. Q. Lou, J. Chem. Phys. 105 (1996) 8699.
[27] Y. F. Liu, Z. Z. Liu, G. S. Lv, Chem. Phys. Lett. 423 (2006) 157.
[28] Y. F. Liu, Y. L. Gao, D. H. Heng, Chem. Phys. 364 (2009) 46.